

State-of-the-Art Imaging of the Placenta

Shital Gandhi¹ · Michael Ohliger² · Liina Poder¹

Published online: 30 October 2015
© Springer Science+Business Media New York 2015

Abstract Abnormalities of the placenta can have long-term implications on fetal and maternal health. Imaging with ultrasound, and sometimes magnetic resonance imaging, is the only means of observing the placenta in vivo, hence playing a significant role in clinical and research efforts for early detection of placental abnormalities. We present a review of placental morphology, imaging appearance of normal placenta and placental abnormalities such as placental implantation disorders and intrauterine growth restriction with emphasis on role of advanced imaging techniques. We hope the review will encourage the readers to give the placenta its much deserved second look.

Keywords Urogenital imaging · Abnormalities · Ultrasound · Placenta · Maternal health

Introduction

Placental abnormalities can have long-term effects on fetal and maternal health. Intrauterine growth restriction (IUGR), prematurity, abnormal fetal neurodevelopment, maternal gestational hypertensive disorders, and gestational diabetes are some of such abnormalities. There is suggestion of

placental involvement in the fetal programming of chronic diseases in adult life such as cardiovascular disease, type 2 diabetes, and certain types of cancer, and that variations in placental morphology could predict some of these diseases [1, 2]. Abnormal placental implantation, a contributor to maternal morbidity, is rising in incidence given increasing number of cesarean sections and uterine surgeries. Unfortunately, a complete understanding of the placenta is fraught with challenges, foremost being inability to adequately study it until after delivery. Lack of adequate animal models has also been an issue [3]. It comes as no surprise that collaborative research initiatives, such as The Human Placenta Project by the National Institute of Child Health and Human Development, have been recently created to foster research efforts to better understand placental development and function with the hope of developing better tools to monitor function in utero, methods for early intervention and improve pregnancy outcomes [3]. Imaging will be central to these research efforts. Ultrasound (US) and magnetic resonance imaging (MRI) are currently the only safe way to visualize placental morphology in vivo. Radiologists therefore need to understand the appearance of normal and abnormal placentas in conditions such as placental implantation disorders, IUGR, and placental masses, as well as state-of-the-art techniques that are being tested or used for evaluation of the placenta, including contrast-enhanced ultrasound, diffusion-weighted imaging (DWI), MR perfusion, MR spectroscopy (MRS), and functional MRI.

Placental Development and Morphology

The placenta constitutes a fetal-derived branching network of villi invading the decidualized endometrium. Villi develop predominantly from trophoblast, which includes cellular cytotrophoblast and acellular syncytiotrophoblast.

This article is part of the Topical Collection on *Urogenital Imaging*.

✉ Shital Gandhi
Shital.gandhi@ucsf.edu

¹ University of California, San Francisco, 350 Parnassus Avenue, San Francisco, CA 94117, USA

² San Francisco General Hospital, 1001 Portero Ave, San Francisco, CA 94110, USA

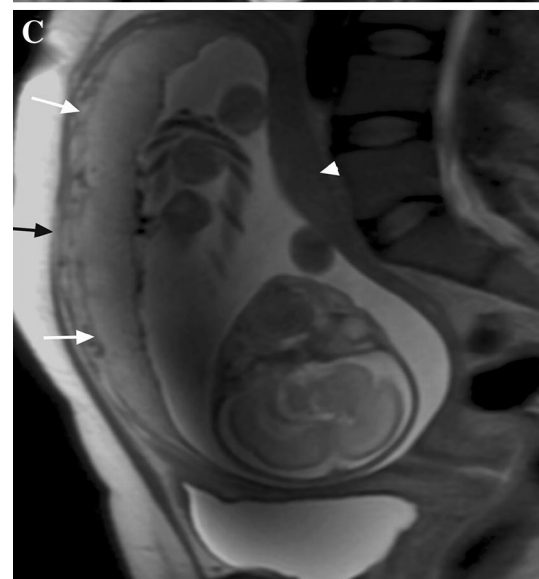
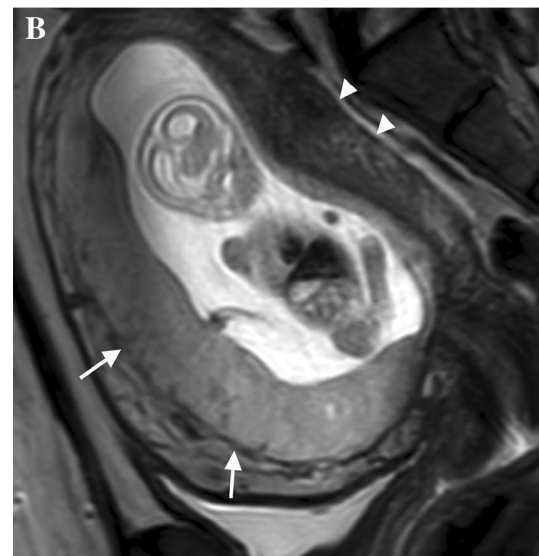
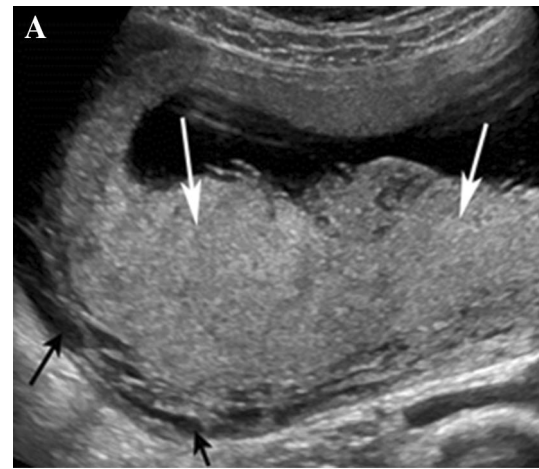
As implantation occurs, lacunar spaces in the syncytiotrophoblast coalesce to form intervillous spaces, which will eventually be bathed in maternal blood forming the prime site of material exchange. Maternal component of the placenta is decidua basalis, which underlies embryonic villi (chorion frondosum) and overlies the placental bed formed by vascularized myometrium containing remodeled uterine spiral arteries and venous sinuses. During the first 8–10 weeks trophoblastic plugging of maternal spiral arteries creates a low oxygen environment protecting the embryo from free radical-mediated teratogenesis. During this time, the intervillous space is filled with plasma filtrate rather than maternal blood. Trophoblast plugs eventually disperse, marking the initiation of utero-placental circulation [4•].

The placenta is a discoid organ measuring 15–20 cm in diameter at term and up to 2.5 cm in thickness [4•]. Amnion covers the fetal surface of placenta (chorionic plate) and the chorionic vessels that branch out in a centrifugal pattern from the umbilical cord insertion. The maternal surface (basal plate) is marked by the presence of raised areas called cotyledons formed by placental septa extending into the intervillous spaces [4•]. The placenta grows more rapidly than the fetus until approximately 20 weeks of gestation, after which the placental thickness in millimeters usually equals the gestational age in weeks ± 10 mm. A thickness of greater than 4 cm is considered abnormal and can be seen in fetal hydrops, gestational diabetes, antepartum infections, and anemia.

Imaging Appearance of the Normal Placenta

Ultrasound

Uniformly echogenic chorionic tissue is visualized by 4 weeks of gestation on gray scale US, followed by the double decidual sac sign. Focal asymmetry at the future site of the placenta can be appreciated as early as 5 weeks, however, it is only after 10–12 weeks of gestation that the placental location is unequivocally visualized i.e., after the chorion laeve has regressed and the endometrial cavity is obliterated. Placentas are uniformly echogenic compared to myometrium. By 14–15 weeks the retroplacental complex is visualized as a hypoechoic layer along the basal plate, consisting of basal decidua, myometrium, and vessels (Fig. 1a). As pregnancy progresses, the placenta becomes more heterogeneous with increased hypoechoic areas. Calcifications within the placenta are normal after 30 weeks of gestation [5]. Intervillous blood flow can be



◀**Fig. 1** Transabdominal transverse ultrasound image through the normal placenta at 20 weeks gestation (**a**), sagittal SSFSE MRI images through the normal anterior placentas of different patients at 22 weeks (**b**) and 27 weeks gestation (**c**) demonstrates homogeneous placentas (*white arrows*) which are hyperintense relative to myometrium on MRI (*arrowheads*). Engorged retroplacental veins are noted as hypoechoic area on ultrasound and flow voids on MRI (*black arrow*). There is marked normal variability in size and number of these veins during different stages of gestation as well as amongst individuals. These should not be mistaken for abnormal vascular flow that occurs in the setting of placental implantation disorders which usually extends into the substance of the placenta and are associated with myometrial thinning

detected as early as 12 weeks on color Doppler US, intraplacental arteries by about 16 weeks, and retroplacental arteries by around 28 weeks [6].

MRI

MRI has better tissue contrast resolution and allows a larger field of view (FOV) providing for evaluation of large patients. Placentas have intermediate signal intensity relative to myometrium on single-shot fast spin-echo (SSFSE) sequences (Fig. 1b, c). Hypo- to isointense signal is noted on steady state free precession sequences (TruFISP/FIESTA) with a relatively ill-defined placental–myometrial interface compared to SSFSE sequence. Placentas are isointense to myometrium on T1-weighted images [7]. In the second trimester, placentas are homogeneous with a smooth flat surface and increased heterogeneity is noted as pregnancy progresses with development of gentle chorionic plate lobulations and better demarcation of cotyledons on T2-weighted images [7, 8]. Cotyledons are more conspicuous on 3T scans [9•]. There is progressive thinning of the myometrium during pregnancy, particularly of the lower uterine segment, which may be difficult to distinguish from abnormal thinning in placental invasion. A matrix size of $256 \times 160/224$ is suggested in addition to a partial phase FOV (0.70–0.75) in axial plane to decrease radiofrequency energy deposition and improve temporal resolution [9•, 10]. At our institution an experienced radiologist supervises all studies performed for placental indications to prescribe plane of imaging and assess adequacy of images.

Safety Issues

There are lack of data suggesting deleterious effects of MRI on the developing human fetus. However, given that deleterious effects have been noted in animal models, caution and risk–benefit assessment by a radiologist is suggested in all pregnant patients referred for MRI irrespective of gestational age. The American College of Radiology guidelines “do not recommend special consideration for first trimester pregnancies” [11]. It is known

that gadolinium contrast agents eventually reach the amniotic fluid, however, the effects of fetal exposure to potentially harmful free gadolinium ions within amniotic fluid are largely unknown. Hence, these contrast agents are mostly contraindicated in pregnant patients unless absolutely essential and after risk–benefit discussion with the patient and referring team [11].

Placental Implantation Disorders

Abnormal adherence of the placenta resulting from direct contact of trophoblastic villi to myometrium without intervening decidual cells has been classified based on depth of invasion into accreta, increta, and percreta, the latter potentially involving adjacent organs, usually the urinary bladder and distal ureter. Separation of this placenta from the uterus can cause life-threatening hemorrhage requiring blood transfusions or emergent hysterectomies. The

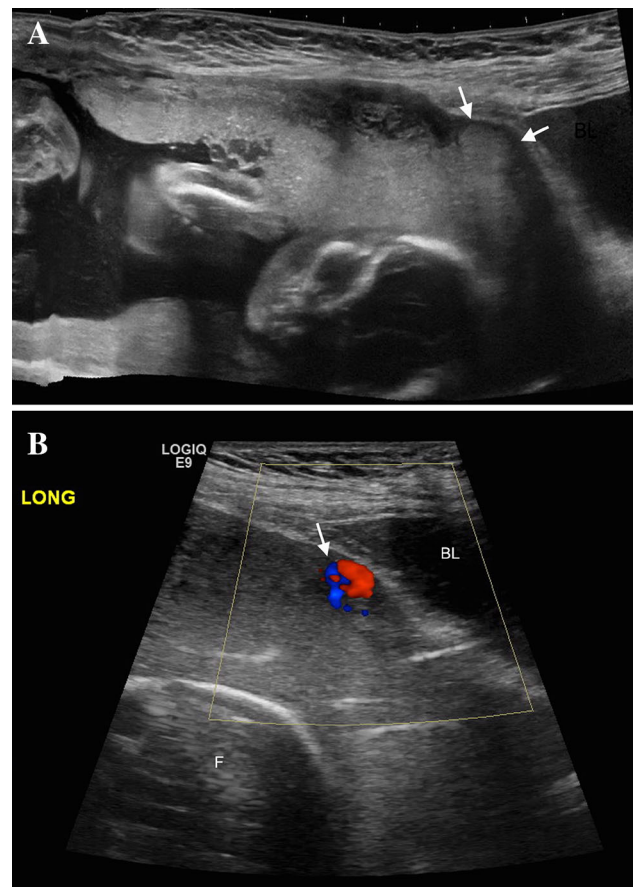


Fig. 2 **a** Transabdominal longitudinal view of anterior placenta with focal placenta accreta in setting of placenta previa and history of two prior cesarean sections demonstrates focal bulging of the placenta in region of myometrial thinning (*arrows*). Of note the placenta is otherwise homogeneous without lacunae. **b** Focal increased vascularity is noted in the region of abnormality at the myometrial–bladder interface

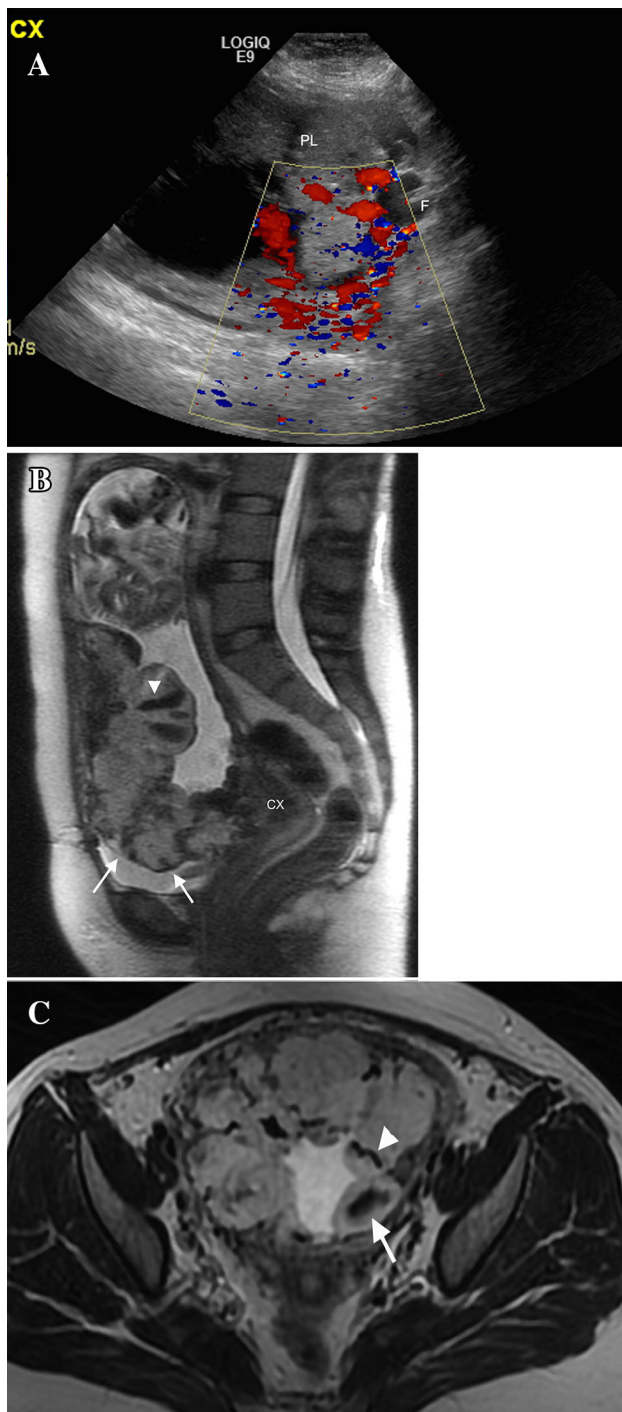


Fig. 3 **a** Transabdominal longitudinal Doppler ultrasound image of a patient with pathologically proven placenta percreta. Increased vascularity within the placenta and at the serosal–bladder interface is noted. Urinary bladder was decompressed by Foley catheter (*F*). **b** Sagittal SSFSE T2-weighted MRI from same patient demonstrates bulging of the lower uterine segment, marked thinning of the myometrium, and suggestion of protrusion of the lobulated placenta into the bladder dome (*arrows*). Marked increased T2 intraplacental bands are noted (*arrowhead*). A partial placenta previa was noted. **c** Axial image through the lower uterine segment again noted T2 intraplacental bands (*arrow*) as well as flow voids extending perpendicular to uterine wall (*arrowhead*), which likely corresponds to similar finding described on US. Patient underwent bilateral uterine artery embolization prior to gravid hysterectomy and partial bladder wall resection

increased desire for uterine sparing modes of management rather than cesarean hysterectomies, stressing upon the need for accurate antenatal detection and description of extent of invasion [13].

Role of Imaging

Ultrasound remains the initial screening modality for placental implantation disorders. Unfortunately, reported diagnostic accuracies of US are highly variable. A meta-analysis of 23 studies involving 3707 pregnancies with history of previous uterine surgery or placenta previa demonstrated a sensitivity of 90.7 % and specificity of 96.9 % for sonographic detection of invasive placentation [14•]. In other small retrospective studies of 58 and 42 patients, lower specificities have been found: 46.5 and 37.5 %, respectively [15, 16]. Bowman et al. noted that when blinded from clinical data, there were significant interobserver variability for diagnosis of placenta accreta with accuracy ranging from 55.9 to 76.4 % [17]. Variability also exists as to which signs are most sensitive or specific. Abnormal vasculature on Doppler ultrasound, particularly increased vascularity at the myometrial–bladder interface (Figs. 2a, b, 3a), was noted to be most accurate by the meta-analysis. Loss of retroplacental clear zone (RCZ) and the presence of multiple placental lacunae had relatively lower sensitivity and specificity. Focal disruption at uterine–bladder interface or frank placental protrusion had highest specificity for prediction of placental invasion (Fig. 3b) [14•]. Increased vascularization perpendicular to uterine wall has been noted to have a high positive predictive value (PPV) [16]. Anterior placental location, grade two or higher placental lacunae (vascular spaces with turbulent flow) (Table 1), and especially loss of RCZ have been noted to be most likely associated with adherent placenta [15, 18]. Rac et al. recently proposed a “Placenta Accreta Index” based on their retrospective experience [19••]. The score included ultrasound parameters of smallest myometrial thickness (less than 1 mm),

presence of placenta previa is an independent risk factor for abnormal placentation. Poor decidualization within a surgical scar is also a strong predisposing factor for abnormal adherence. In a patient with placenta previa, the risk is noted to be 11, 40, and 60 % with a history of 1, 2, and 3 or more prior cesarean sections, respectively [12]. Planned delivery of patients with adherent placentas reportedly decreases morbidity and blood loss [13]. In addition, there is an

Table 1 Grading of placental lacunae on ultrasound based on number and morphology [18]

Grade 0	None
Grade 1	1–3, generally small
Grade 2	4–6, irregular and larger
Grade 3	Many large and bizarre shaped (swiss-cheese appearance)

Table 2 Summary of US findings seen in setting of abnormal placenta [14•, 15–18, 19••, 20, 21••]

US findings
Placenta previa
Anterior placental location
Increased heterogeneity
Increased number and size of placental lacunar spaces with turbulent flow
Loss of normal retroplacental hypoechoic zone
Decreased retroplacental myometrial thickness (<1 mm)
Abnormal intraplacental vascularity (bridging vessels)
Increased vascularity at the myometrial–bladder interface
Focal disruption of myometrial–bladder interface or frank protrusion into urinary bladder

Table 3 Summary of MRI findings in setting of abnormal placenta [9•, 12, 21••, 22–25, 26•]

MRI findings
Placenta previa
Anterior placental location
Bulging of the lower uterine segment
Increased heterogeneity on T2W imaging
Presence of T2 dark intraplacental bands
Focal interruption in myometrial wall
Tenting of urinary bladder
Bulging of the placenta into internal os

lacunar spaces, the presence of bridging vessels, and placental location along with history of prior cesarean section. The highest value (suggesting greatest risk) was assigned to the presence of grade 3 lacunae and history of 2 or more cesarean sections. Another scoring system comprising gray scale findings such as length of loss of RCZ and number of lacunae has been reported to be useful for antenatal risk assessment of maternal complications [20].

MRI has been increasingly used for problem solving and better characterization of depth of invasion in suspected placenta percreta. In a recent meta-analysis involving 1010 pregnancies, MRI was noted to be 94.4 % sensitive and 84 % specific for detection of abnormal placenta [21••]. Four studies comparing the accuracies of MRI and US yielded no significant difference for detection of invasive



Fig. 4 **a** Sagittal T2 FSE image of uterus in a woman with history of five cesarean sections demonstrates marked myometrial thinning adjacent to a heterogeneous anterior placenta in region of cesarean section scar (*arrows*) without definite urinary bladder invasion. This was pathology proven transmural placental invasion without percreta. The low-lying gestational sac containing a non-viable fetus (*F*) extends through the cervical canal consistent with abortion in progress. Blood products fill the vagina (*V*). **b** Single sagittal early arterial phase image from dynamic post gadolinium series demonstrates relatively early enhancement of trophoblastic tissue compared to myometrium allowing for better visualization of placental invasion (*arrows*)

placenta [22]. The above meta-analysis noted lower uterine bulging, heterogeneous signal intensity, T2 dark intraplacental bands (possibly represent fibrin deposition), focal interruption of myometrium, and tenting of urinary

bladder to all be fairly accurate (Fig. 3b, c). This is similar to a small retrospective review by Lax et al. and a 85 % PPV of uterine bulging noted by Riteau et al., which increased to 90 % with addition of T2 dark intraplacental bands [16, 22]. Placental protrusion into the internal os in the setting of placenta previa was noted to be a good additional sign of abnormal invasiveness by a recent retrospective review [23]. A summary of US and MRI findings are listed in Tables 2 and 3, respectively.

In our experience, placing a Foley catheter is helpful to control distension of urinary bladder in cases with high suspicion for percreta. Besides the T2-weighted sequences routinely obtained, a T1-weighted sequence with fat saturation is suggested for detection of hemorrhage. There are very limited data regarding the use of DWI for diagnosis of placental invasion. One small study noted that the placenta is markedly restricted on DWI at high *b*-value (1000 s/mm²) allowing for good placental–myometrial differentiation. Fusion data extrapolated from B0 and B1000 images helped accurately identify myometrial thickness in this small study [24]. Use of gadolinium has been proposed in the past as a means to better define the placenta. However, given safety concerns it is not routinely used, unless the fetus is known to be non-viable and/or patient is pre-surgical (Fig. 4a, b).

Studies have shown better outcomes when care is provided at a center with multidisciplinary expertise and experience, irrespective of type of treatment [25, 26]. Our institution is one such center and to that effect a monthly interdisciplinary meeting is held to discuss cases, attended by various specialties including radiology, pathology, and anesthesiology in addition to maternal-fetal medicine specialties.

Intrauterine Growth Restriction (IUGR) and Pregnancy-Induced Hypertension (PIH)/Preeclampsia (PE)

Abnormal utero-placental blood flow is thought to be the underlying abnormality in most IUGR and at least early PIH/PE cases, potentially related to abnormal trophoblast plugging, incomplete remodeling of maternal spiral arteries, and increased early villous oxidative stress. Doppler evaluation of maternal uterine and fetal umbilical arteries offer an indirect evaluation of the utero-placental resistance and are currently used in clinical practice. Direct non-invasive qualitative and quantitative assessment of placental perfusion can further increase our understanding of this complex process, enable early detection of at-risk fetuses, and potentially help monitor response to intervention. Multiple efforts have been made in this direction as described below.

Ultrasound

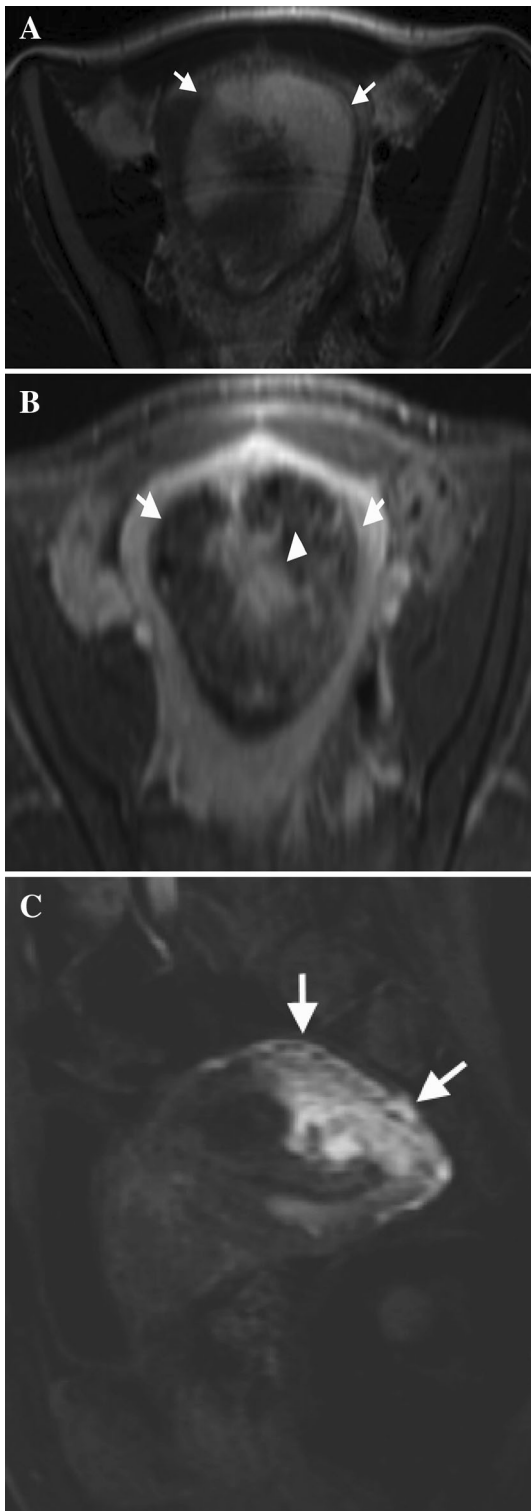
3-D power-Doppler US has been used to calculate placental bed vascularization index (VI) by measuring the number of color voxels relative to gray voxels in the assigned region. In a study involving 4325 low-risk women at 11–14 weeks, VI was superior to first trimester sonographic or biochemical markers to predict severe PE and severe pregnancy problems including combination of PE and IUGR. It was as good as second trimester uterine artery Doppler pulsatility index (UAPI) for prediction of poor outcome [27]. A more recently published prospective study used 3-D US to calculate placental volume in conjunction with UAPI at 11–13 weeks gestation. Placental volume was smaller and UAPI was higher in patients who developed early PIH compared to unaffected population (combined detection rate for early PIH being 67.5 % with 5 % false positive). This was not seen in patients with late PIH, which is consistent with suspected differences in pathophysiology and fetal outcomes for early versus late onset PE, though not yet definitively proven [28, 29].

Advanced US Techniques

We found only one remote study using intravascular US contrast agent (Levovist microbubble) to evaluate utero-placental circulation. The group also reported lack of adverse pregnancy outcomes suggesting these agents are safe [30, 31]. However, this involved a small number of patients and lacked quantitative data, which has been provided by animal studies [32]. Recent reports describe use of in vivo shear wave elastography and note significant higher placental stiffness in patients with PE [33, 34]. More data are required to establish utility and safety of these techniques.

MRI

A thickened, globular placenta with higher maximal thickness to placental volume ratios is associated with increase perinatal mortality in IUGR patients in one study of placental phenotype on MRI. Normal placentas were disk like with tapering edges. A higher percentage of abnormal placental volume on T2-weighted images (including infarcts and hemorrhage) significantly correlated with severity of IUGR predicting perinatal mortality [35]. A retrospective analysis of dynamic post-contrast MRI obtained for placental invasion noted patchy enhancement with underperfused areas, significantly lower maximum signal intensity reflecting maternal hypoperfusion and greater variation of intervillous flow throughout the placenta in patients with IUGR. The authors suggested a role



◀**Fig. 5** a, b Axial T2-weighted and T1 post-contrast images demonstrate an expanded uterine cavity filled with a complete mole and relatively intact myometrium (*arrows*). Small cysts are noted on the T2-weighted image. On post-contrast images the thin walls enhance and surround non-specific enhancing tissue (*arrowhead*). c Single sagittal image from a dynamic post-contrast study performed on a different patient with invasive mole. Even though myometrial enhancement is not specific for invasion and can be seen in setting of retained products of conception, early images from a dynamic study can help delineate the extent of abnormality and exclude extrauterine involvement as seen in this retroverted uterus with invasive mole corresponding to full thickness enhancement of the fundal myometrium adjacent to focal endometrial enhancement (*arrows*)

Advanced MRI Techniques

Most research using advanced MRI techniques to evaluate placental pathophysiology has been performed on animals, description of which is beyond the scope of this article. Instead, we present a summary of few recent investigations using these techniques to provide the reader with a glimpse of where we stand and what the future may behold.

Evaluation of placental perfusion An ideal technique would not require intravenous gadolinium-based contrast. Derwig et al. applied two such techniques to obtain quantitative placental perfusion measures, namely arterial spin labeling (ASL) using the flow sensitive alternating inversion recovery (FAIR) technique and intravoxel incoherent motion (IVIM) echoplanar imaging on a 1.5 Tesla magnet. Statistically significant decreased perfusion was observed in women with small for gestational age fetuses (SGA) versus appropriate for gestational age fetuses and this decrease correlated with increased uterine artery pulsatility index in SGA fetuses obtained by ultrasound Doppler evaluation [37]. In a more recently published study, Sohlberg et al. calculated perfusion fraction of placentas of normal and preeclampsia pregnancies using IVIM analysis of diffusion-weighted echo planar imaging. They found that the perfusion fraction was smaller in early onset preeclampsia (prior to 34 weeks) and larger in late onset preeclampsia compared to that noted in normal pregnancies. In addition, a decrease in perfusion fraction by 0.7 % per week was noted in the 22 normal pregnant patients studied [38].

Evaluation of placental oxygenation Blood oxygenation level-dependent (BOLD) MRI currently provides the only non-invasive means to directly evaluate placental and fetal tissue oxygenation. This technique exploits the endogenous contrast created by different magnetic properties of oxy- and deoxy-hemoglobin. In a study of eight healthy pregnant women in their second trimester, an oxygen challenge resulted in increased homogeneity and increased overall signal within the placenta on BOLD MRI [39]. In addition,

of vasospasm and potential use of vasodilators for treatment of these patients [36]. However, given safety concerns we are not sure if gadolinium agents will be used in routine clinical practice in the near future.

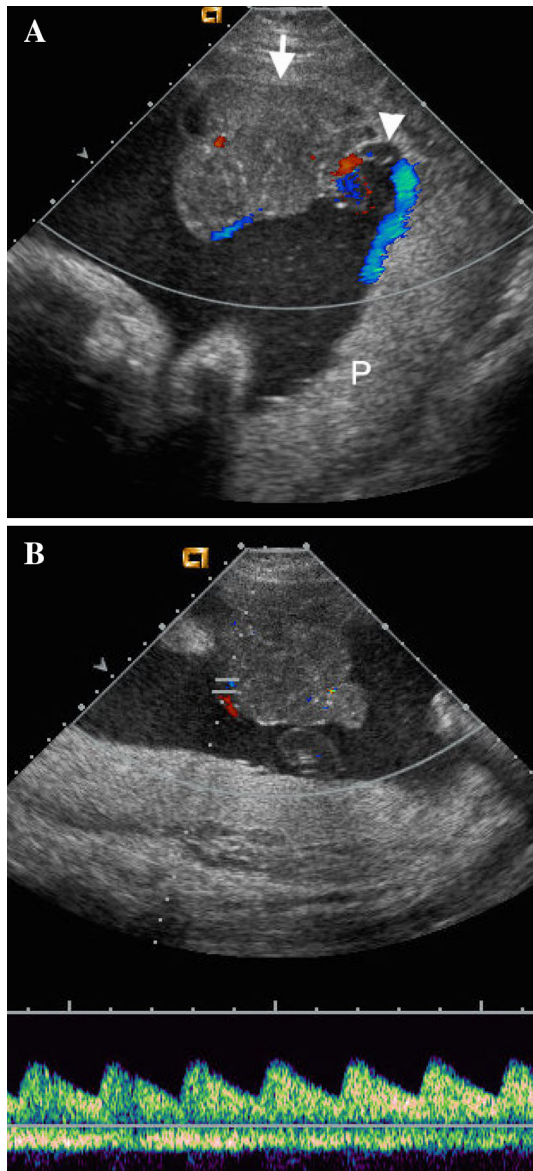


Fig. 6 **a** Transabdominal view of hypoechoic well-circumscribed placental mass (*arrow*), adjacent to cord insertion (*arrowhead*). Most of the placenta (*P*) is posterior and relatively more echogenic. **b** Detection of vascularity contiguous with fetal circulation can help differentiate from placental teratomas, degenerating fibroids, or hematomas

the investigators noted an increase in BOLD MRI signal in fetal liver, spleen, and kidneys after hyperoxic challenge, as opposed to no change in fetal brain oxygenation prior, during, or after the challenge. The authors concluded that this was a reflection of normal auto regulation of fetal cerebral circulation ('reversed' brain sparing) [40]. This technique has been applied to animal IUGR models, where compromised placentas were noted to have reduced response to oxygen challenge. No published studies

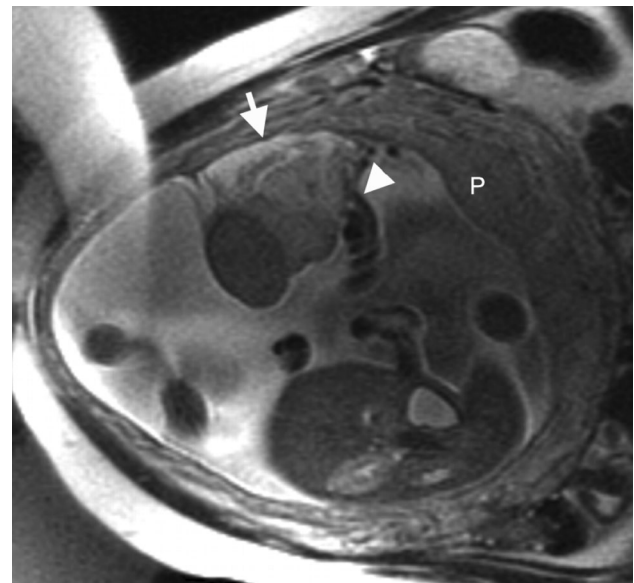


Fig. 7 Axial SSFSE image of heterogeneous placental mass (*arrow*) with hyperintense component relative to placenta (*P*) and adjacent to cord insertion (*arrowhead*)

evaluating maternal oxygen challenge in human pregnancies with known IUGR are noted to date.

Evaluation of placental diffusion Role of DWI in evaluating placental invasion has already been described. A recent case control study of pregnant women using diffusion tensor imaging to quantify functional placental tissue noted an almost threefold decrease in volume of functional tissue in placental-IUGR patients compared to controls. Mean diffusivity and fractional anisotropy measures were also significantly reduced [41].

Evaluation of placental metabolism ^{31}P magnetic resonance spectroscopy (MRS) has been used to study placental function. One of the largest in vivo studies noted a higher phosphodiesterase (PDE) to phosphomonoesterase (PME) spectral intensity ratio in patients with early onset preeclampsia compared to gestational age-matched controls. PDE represents cell membrane degradation products and the increase in early onset preeclampsia likely correlates with placental apoptosis noted in these patients [42].

Gestational Trophoblastic Disease (GTD)

GTD is a spectrum of diseases, which include genetically abnormal conceptions with neoplastic potential i.e., complete (CHM) and partial (PHM) hydatidiform moles and gestational trophoblastic neoplasms (GTN), such as invasive moles and choriocarcinoma. These diseases are rare, with a prevalence of upto 1 per 1000 for hydatidiform moles, which constitute 80 % of GTD's [4•]. Risk factors

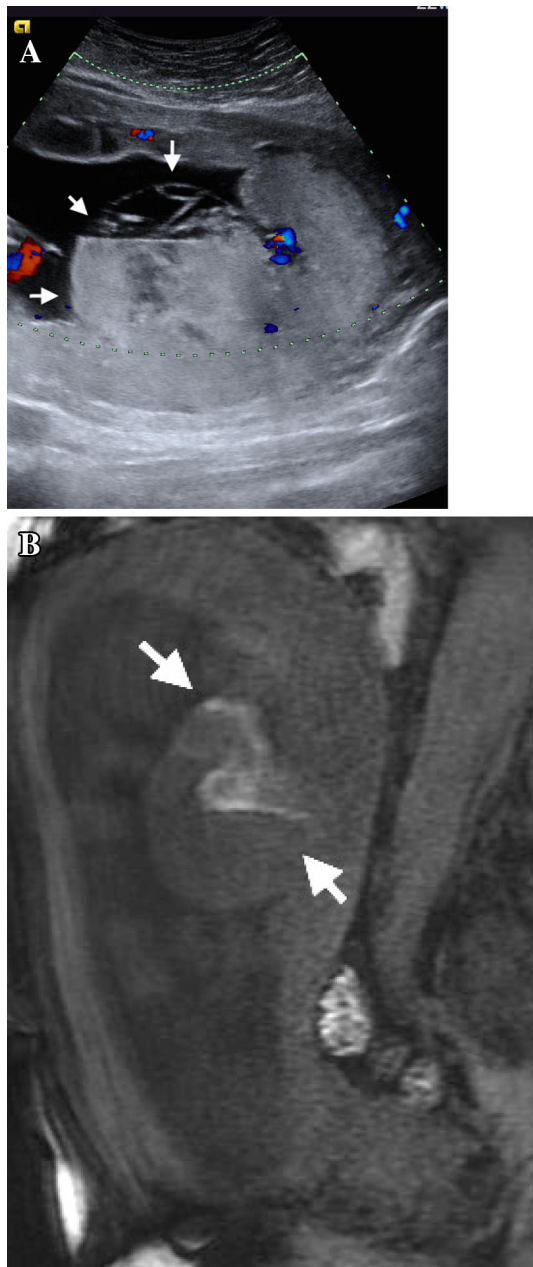


Fig. 8 **a** Transabdominal sonogram demonstrates a placental mass (arrows) with fluid–fluid level and complex architecture mimicking a teratoma. **b** Sagittal T1 with fat saturation demonstrates hyperintensity (arrows) within the mass suggesting hemorrhage. Lack of intrinsic fat or large calcifications made teratoma a much less likely diagnosis. Final pathology confirmed chorioangioma

include extremes of maternal age and prior history of molar pregnancy [43]. The availability of effective chemotherapeutic regimens and a highly sensitive biomarker, beta-human chorionic gonadotrophin (b-hCG), has dramatically improved survival rates for these patients [43]. Ultrasound remains the primary imaging modality, one of its crucial roles being exclusion of normal pregnancy as a cause of

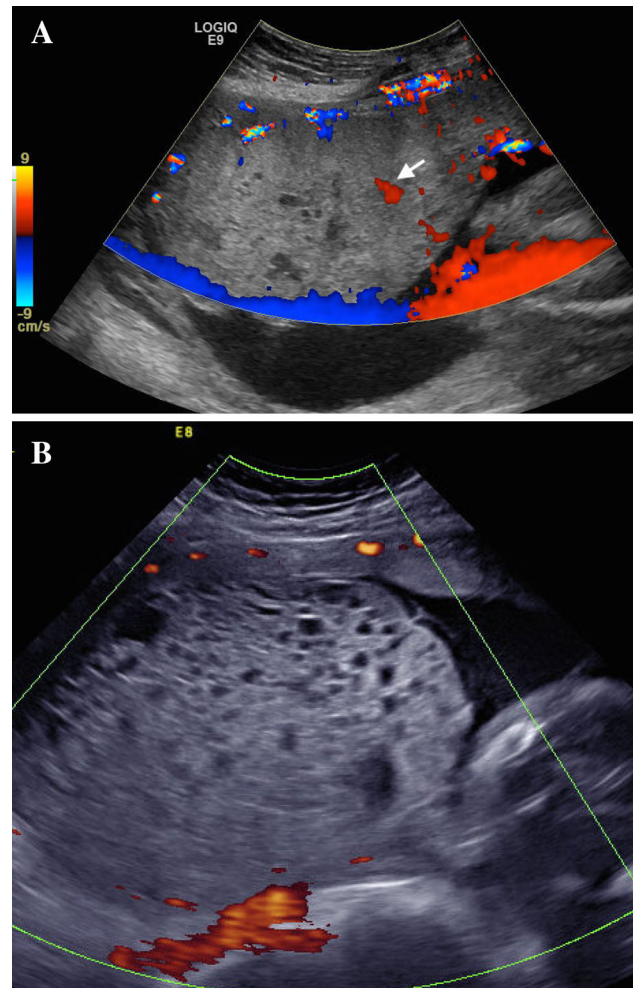
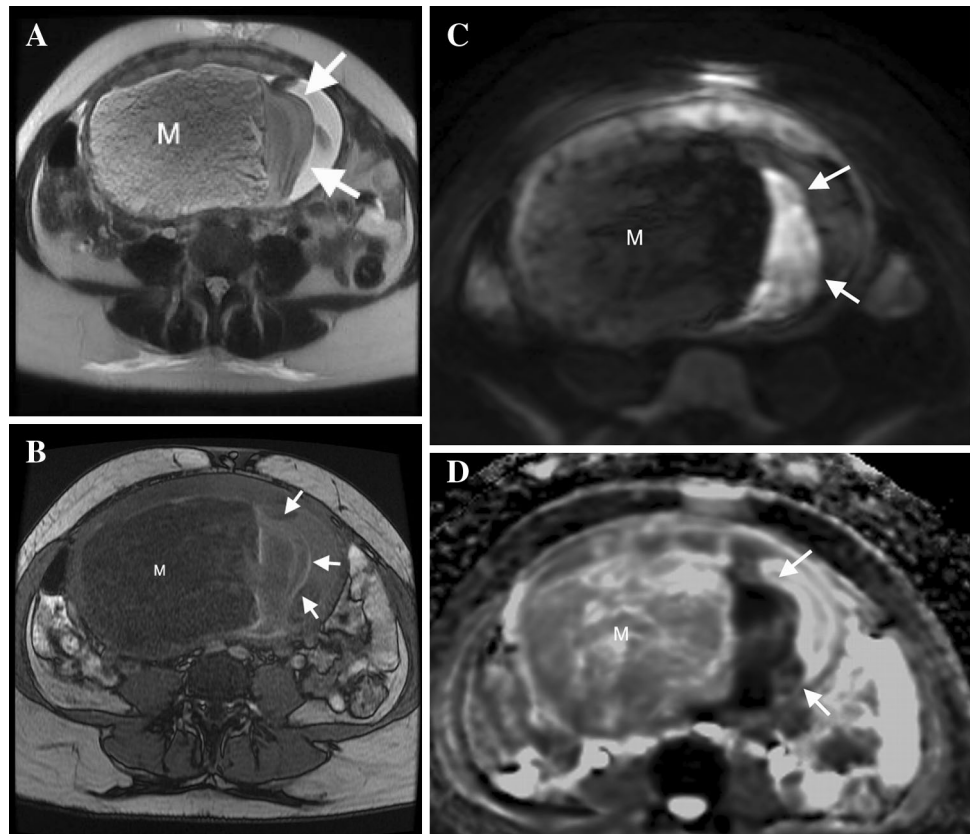


Fig. 9 **a** Slow flow detected (arrow) in some cystic spaces noted in this placental mass in keeping with postnatal diagnosis of placental mesenchymal dysplasia (PMD). **b** No flow is detected in the hypodic villi of a complete mole in this case

elevated b-hCG. Distinction between types of HM is important as 15 % of CHM have invasive potential compared to only 0.5 % of PHM [4•]. The classic description of CHM is an enlarged uterus without visible fetal parts, heterogeneous echoes produced by tiny cysts within the endometrial cavity (“snowstorm” appearance), which progressively increase in size (“cluster of grapes”). PHM has a thickened placenta with non-uniform cysts in conjunction with a normal or abnormal appearing fetus, which can resemble a hydropic placenta associated with spontaneous abortion [44–46]. These findings along with the presence of theca-lutein ovarian cysts are now less frequently seen [44, 47]. First trimester sonographic appearance of HM is now commonly indistinguishable from a failed early pregnancy, missed or incomplete abortion. In these cases, molecular genotyping of evacuated products of conception can be used for definitive diagnosis.

Fig. 10 Patient with CHMTF and normal twin presented with vaginal bleeding in third trimester. Ultrasound showed no evidence of hemorrhage. **a** Axial SSFSE demonstrates large multicystic mass (*M*) separate from the anterior placenta with layering blood products along the left margin (*arrows*). **b** This was a subtle finding on Axial T1 (*arrows*) along the left margin of the mass (*M*). **c, d** Subchorionic hematoma was more obvious as restricted diffusion (*arrows*) on b500 diffusion-weighted image (c) and apparent diffusion coefficient (ADC) (d) along the edge of known CHMTF (*M*)



Interestingly, a recent study noted that earlier detection of HM did not change incidence of post-molar GTN's [47]. The presence of focal myometrial involvement or retained endometrial tissue on the first follow-up exam after evacuation has been reported to be predictive of GTN, even before diagnosis can be made by beta-hCG levels. The presence of indistinct junctional zone with hypervascularity was not predictive [48]. Pelvic MRI is used for problem solving and evaluation of local extension. The appearance of HM has been previously described as T1 hypointense, T2 hyperintense, enhancing heterogeneous multicystic tissue within an enlarged uterus (Fig. 5a–c) [9•]. MRI is also noted to be superior to US for evaluating myometrial extension [9•]. To our knowledge, no recent data exist regarding use and accuracy of advanced MRI techniques for evaluation of GTD.

Non-trophoblastic Placental Masses

Chorioangioma is the most common benign placental neoplasm occurring in up to 1 % of pregnancies. On gray scale US, these are well-circumscribed hypoechoic masses with varying heterogeneity and cystic change, sometimes with calcifications, bulging from the chorionic surface and usually located close to the umbilical cord insertion (Fig. 6a) [49]. Substantial vascularity or single feeding

vessel contiguous with fetal circulation can help differentiate from placental teratoma, degenerating fibroid, hematomas, and placental mesenchymal dysplasia (Fig. 6b) [49]. On MRI, these are generally T1 isointense with variable usually hyperintense T2 signal (Fig. 7). Lesions greater than 4–5 cm are more likely to be associated with complications related to polyhydramnios, preterm labor, non-immune fetal hydrops, fetal anemia, thrombocytopenia, growth retardation, and sudden infant death [49, 50]. Favorable outcome with giant chorioangiomas (11 cm) with close surveillance and amniocentesis has been recently reported [51]. Sonographic guidance for amniocentesis and intrauterine transfusion for fetal anemia is performed in some centers to manage these patients. Placental teratomas are extremely rare benign tumors with favorable outcome. They are heterogeneous and internal calcifications and fat can be confirmed on US or MRI. Sonographic appearance can be mistaken for fetal neck mass or acardiac twin, the latter being distinguished by the presence of organized tissue and separate umbilical cord [52]. Most placental masses are well characterized on US, however MRI can be a problem-solving tool for atypical appearing cases (Fig. 8a, b).

Placental mesenchymal dysplasia (PMD) is a rare vascular anomaly first described in 1991 and is likely under-reported [53]. In a recent systematic review of 64 cases,

80 % had a cystic placenta with hypoechoic areas ('molar' or 'swiss-cheese' appearance), 50 % had an enlarged and/or focally thickened placenta and 16 % had dilated chorionic vessels, sometimes described as aneurysmal [53]. Morphologic changes can start as early as 13 weeks of gestation. Ohira et al. reported gradual decreased size of vesicular lesions on serial ultrasound and MR as pregnancy advances. Aneurysmal dilation of chorionic vessels was noted to be a late finding, never seen before 25 weeks gestation in their experience [54]. Reported concurrent fetal abnormalities include Beckwith–Wiedmann syndrome in 19–23 % cases, other aneuploidies and hepatic mesenchymal tumors, in addition to association with preterm delivery and IUGR [53, 54]. Only 9 % of pregnancies were uncomplicated in the systematic review described above [53]. Hence, careful assessment and surveillance of associated fetus is warranted.

PMD and partial mole have similar imaging appearances. The presence of a morphologically normal fetus in PMD can help distinguish from abnormal triploid fetus in partial mole that usually does not survive into the second trimester. Serum b-hCG levels are unreliable as they can be elevated in 38 % of PMD cases. A volume analysis technique called inversion mode has been used for 3-D sonographic visualization and better characterization of fluid-filled structures [55]. One group reported a 'stained-glass' sign describing the color Doppler appearance of PMD using very low pulse repetition frequency setting to observe slow flow of differing velocities within dilated vessels. No flow is expected in the hydropic villi of molar tissue (Fig. 9a, b) [56].

Another entity that is sometimes difficult to distinguish from PMD on early prenatal US is complete hydatidiform mole with twin live fetus (CHMTF). Both entities are multicystic on US. Location is one of the most important differentiating factors as CHMTF arising from one of the fertilized eggs develops outside the sac of the normal dizygotic twin, which has a separate normal placenta. PMD on the other hand develops from the same egg as the fetus and hence no separate placenta is noted [57, 58]. Larger field of view and multiplanar capability of MRI enables better visualization of location compared to US in some cases. In addition, excellent tissue characterization of MRI enables detection of hemorrhage, which is not uncommon in molar pregnancy and currently unreported in PMD (Fig. 10) [58]. In our experience, acute hemorrhage is more conspicuous on diffusion-weighted images compared to relative isointensity on T1W images (Fig. 10) [59•]. However, we cannot reliably claim hemorrhage to be specific for CHMTF given rarity of these entities and limited reported experience.

Conclusion

The placenta has been and remains one of the least understood human organs. Recent increased interest in the placental role in fetal and maternal well-being behooves radiologists to carefully observe the placenta in normal and abnormal states, keep up-to-date with evolving advanced US and MRI techniques which may be widely used in clinical practice in the near future, and encourage multi-disciplinary collaboration to improve patient outcomes, further knowledge, and promote research.

Compliance with Ethics Guidelines

Conflict of Interest Shital Gandhi, Michael Ohliger, and Liina Poder each declare no potential conflicts of interest.

Human and Animal Rights and Informed Consent This article does not contain any studies with human or animal subjects performed by any of the authors.

References

Papers of particular interest, published recently, have been highlighted as:

- Of importance
- Of major importance

1. Barker DJP, Thornburg KL. Placental programming of chronic disease, cancer and lifespan: a review. *Placenta*. 2013;34:841–5.
2. Tarrade A, Panchenko P, Junien C, et al. Placental contribution to nutritional programming of health and diseases: epigenetics and sexual dimorphism. *J Exp Biol*. 2015;218:50–8.
3. Guttmacher AE, Maddox YT, Spong CY. The Human Placenta Project: placental structure, development, and function in real time. *Placenta*. 2014;35:303–4.
4. • Benirschke K, Burton GJ, Baergen RN. Pathology of the human placenta. 6th ed. Berlin: Springer; 2012. *Good resource for understanding placental anatomy and pathophysiology.*
5. Bowman ZS, Kennedy AM. Sonographic appearance of the placenta. *Curr Probl Diagn Radiol*. 2014;43:356–73.
6. Moran M, AcAuliffe F. Imaging and assessment of placental function. *J Clin Ultrasound*. 2011;39:390–8.
7. Victoria T, Johnson AM, Kramer SS, et al. Extrafetal findings at fetal MR: evaluation of the normal placenta and correlation with ultrasound. *Clin Imaging*. 2011;35:371–7.
8. Nguyen D, Nguyen C, Yacobozzi M, et al. Imaging of the placenta with pathologic correlation. *Semin Ultrasound CT MR*. 2012;33:65–77.
9. • Masselli G, Gualdi G. MR imaging of the placenta: what a radiologist should know. *Abdom Imaging*. 2013;38:573–87. *Good review of routine MRI placental imaging from group that studied role of DWI in placental abruption.*
10. Elsayes KM, Trout AT, Friedkin AM, et al. Imaging of the placenta: a multimodality pictorial review. *Radiographics*. 2009;29:1371–91.

11. Kanal E, Barkovich AJ, Bell C, et al. ACR guidance document on MR safe practices: 2013. *J Magn Reson Imaging*. 2013;37:501–30.
12. Silver RM, Landon MB, Rouse DJ, et al. Maternal morbidity associated with multiple cesarean deliveries. *Obstet Gynecol*. 2006;107:1226–32.
13. Fox KA, Shamshirsaz AA, Carusi D, et al. Conservative management of morbidly adherent placenta: expert review. *Am J Obstet Gynecol*. 2015;. doi:[10.1016/j.ajog.2015.04.034](https://doi.org/10.1016/j.ajog.2015.04.034).
14. • D'Antonio F, Iacovella C, Bhide A. Prenatal identification of invasive placentation using ultrasound: systematic review and meta-analysis. *Ultrasound Obstet Gynecol*. 2013;42:509–17. *The largest meta-analysis that we know of*.
15. Tanimura K, Yamasaki Y, Ebina Y, et al. Prediction of adherent placenta in pregnancy with placenta previa using ultrasonography and magnetic resonance imaging. *Eur J Obstet Gynecol Reprod Biol*. 2015;187:41–4.
16. Riteau AS, Tassin M, Chambon G, et al. Accuracy of ultrasonography and magnetic resonance imaging in the diagnosis of placenta accreta. *PLoS One*. 2014;9(4):e94866. doi:[10.1371/journal.pone.0094866](https://doi.org/10.1371/journal.pone.0094866).
17. Bowman ZS, Eller AG, Kennedy AM, et al. Interobserver variability of sonography for prediction of placenta accreta. *J Ultrasound Med*. 2014;33:2153–8.
18. Finberg HJ, Williams JW. Placenta accreta: prospective sonographic diagnosis in patients with placenta previa and prior cesarian section. *J Ultrasound Med*. 1992;11:333–43.
19. •• Rac MW, Dashe JS, Wells CE et al. Ultrasound predictors of placental invasion: the Placenta Accreta Index. *Am J Obstet Gynecol*. 2015;212:343. doi:[10.1016/j.ajog.2014.10.022](https://doi.org/10.1016/j.ajog.2014.10.022). *Authors develop an index stratifying risk of placental invasion based on clinical and imaging criteria which could be applicable in a clinical setting*.
20. Gilboa Y, Spira M, Mazaki-Tovi S, et al. A novel sonographic scoring system for antenatal risk assessment of obstetric complications in suspected morbidly adherent placenta. *J Ultrasound Med*. 2015;34:561–7.
21. •• D'Antonio F, Iacovella C, Palacios-Jaraquemada J et al. Prenatal identification of invasive placentation using magnetic resonance imaging: systematic review and meta-analysis. *Ultrasound Obstet Gynecol*. 2014;44:8–16. *The only recent meta-analyses and one of the few systematic reviews pertaining to MRI diagnosis of placental invasion*.
22. Lax A, Prince MR, Mennitt KW, et al. The value of specific MRI features in the evaluation of suspected placental invasion. *Magn Reson Imaging*. 2007;25:87–93.
23. Ueno Y, Kitajima K, Kawakami F, et al. Novel MRI finding for diagnosis of invasive placenta praevia: evaluation of findings for 65 patients using clinical and histopathological correlations. *Eur Radiol*. 2014;24:881–8.
24. Morita S, Ueno E, Mikihiko F, et al. Feasibility of diffusion-weighted MRI for defining placental invasion. *J Magn Reson Imaging*. 2009;30:666–71.
25. Shamshiraz AA, Fox KA, Salmanian B, et al. Maternal morbidity in patients with morbidly adherent placenta treated with and without a standardized multidisciplinary approach. *Am J Obstet Gynecol*. 2015;212:218.e1–9. doi:[10.1016/j.ajog.2014.08.019](https://doi.org/10.1016/j.ajog.2014.08.019).
26. • Silver RM, Fox KA, Barton JR et al. Center of excellence for placenta accreta. *Am J Obstet Gynecol*. 2015;212:516–8. *Good review that summarizes findings of placental invasion and describes data supporting care of women with placental invasion at centers of excellence*.
27. •• Hafner E, Metzzenbauer M, Stümpflen I et al. Measurement of placental bed vascularization in the first trimester, using 3D-power-doppler, for the detection of pregnancies at-risk for fetal and maternal complications. *Placenta*. 2013;34:892–8. *Study involving large number of first trimester women (4325) showing that evaluation of placental bed vascularity can predict severe pregnancy problems in first trimester*.
28. • Arakaki T, Hasegawa J, Nakamura M et al. Prediction of early- and late- onset pregnancy-induced hypertension using placental volume on 3-D ultrasound and uterine artery Doppler. *Ultrasound Obstet Gynecol*. 2015;45:539–43. doi:[10.1002/uog.14633](https://doi.org/10.1002/uog.14633). *Interesting use of 3-D imaging technique for evaluation of placental vascularity*.
29. Arakaki T, Hasegawa J, Nakamura M, et al. Re: prediction of early- and late-onset pregnancy-induced hypertension using placental volume on 3-D ultrasound and uterine artery Doppler. *Ultrasound Obstet Gynecol*. 2015;45:513. doi:[10.1002/uog.14857](https://doi.org/10.1002/uog.14857).
30. Ordén MR, Gudmundsson S, Kirkinen P. Intravascular ultrasound contrast agent: an aid in imaging intervillous blood flow? *Placenta*. 1999;20:235–40.
31. Ordén MR, Leinonen M, Kirkinen P. Contrast-enhanced ultrasonography of uteroplacental circulation does not evoke harmful CTG changes or perinatal events. *Fetal Diagn Ther*. 2000;15:139–45.
32. Arthuis CJ, Novell A, Escoffre JM, et al. New insights into uteroplacental perfusion: quantitative analysis using Doppler and contrast-enhanced ultrasound imaging. *Placenta*. 2013;34:424–31.
33. Kilic F, Kayadibi Y, Yuksel MA, et al. Shear wave elastography of placenta: in vivo quantification of placental elasticity in preeclampsia. *Diagn Interv Radiol*. 2015;21:202–7.
34. Cimsit C, Yoldemir T, Akpınar IN. Shear wave elastography in placental dysfunction: comparison of elasticity values in normal and preeclamptic pregnancies in second trimester. *J Ultrasound Med*. 2015;34:151–9.
35. • Damodaram M, Story L, Eixarch E et al. Placental MRI in intrauterine fetal growth restriction. *Placenta* 2010;31:491–8. *Interesting observations of placental morphology on MRI that needs further validation*.
36. Brunelli R, Masselli G, Parasassi T, et al. Intervillous circulation in intra-uterine growth restriction. Correlation to fetal well being. *Placenta*. 2010;31:1051–6.
37. Derwig I, Lythgoe DJ, Barker GJ, et al. Association of placental perfusion, as assessed by magnetic resonance imaging and uterine artery Doppler ultrasound, and its relationship to pregnancy outcome. *Placenta*. 2013;34:885–91.
38. Sohlberg S, Mulic-Lutvica A, Lindgren P, et al. Placental perfusion in normal pregnancy and early and late preeclampsia: a magnetic resonance imaging study. *Placenta*. 2014;35:202–6.
39. Sorensen A, Peters D, Frund E, et al. Changes in human placental oxygenation during maternal hyperoxia estimated by blood oxygen level-dependent magnetic resonance imaging (BOLD MRI). *Ultrasound Obstet Gynecol*. 2013;42:310–4.
40. Sorensen A, Peters D, Simonsen C, et al. Changes in human fetal oxygenation during maternal hyperoxia as estimated by BOLD MRI. *Prenat Diagn*. 2013;33:141–5.
41. Javor D, Nasel C, Schweim T, et al. In vivo assessment of putative functional placental tissue volume in placental intrauterine growth restriction (IUGR) in human fetuses using diffusion tensor magnetic resonance imaging. *Placenta*. 2013;34:676–80.
42. Sohlberg S, Wikstrom A-K, Olovsson M, et al. In vivo ³¹P-MR spectroscopy in normal pregnancy, early and late preeclampsia: a study of placental metabolism. *Placenta*. 2014;35:318–23.
43. Seckl MJ, Sebire NJ, Fisher RA, et al. Gestational trophoblastic disease: ESMO Clinical Practice Guidelines for diagnosis, treatment and follow up. *Ann Oncol*. 2013;24(6):vi39–50.
44. Lazarus E, Hulka C, Siewart B, et al. Sonographic appearance of early complete molar pregnancies. *J Ultrasound Med*. 1999;18:589–94.

45. Kani KK, Lee JH, Dighe M, et al. Gestational trophoblastic disease: multimodality imaging assessment with special emphasis on spectrum of abnormalities and value of imaging in staging and management of disease. *Curr Probl Diagn Radiol*. 2012;41:1–10.
46. Dhanda S, Ramani S, Thakur M. Gestational trophoblastic disease: a multimodality imaging approach with impact on diagnosis and management. *Radiol Res Pract*. 2014;2014:842751. doi:[10.1155/2014/842751](https://doi.org/10.1155/2014/842751).
47. Sun SY, Melamed A, Goldstein DP, et al. Changing presentation of complete hydatidiform mole at the New England Trophoblastic Disease Center over the past three decades: does early diagnosis alter risk for gestational trophoblastic neoplasia? *Gynecol Oncol*. 2015;138:46–9.
48. Malek M, Moradi B, Mousavi AS, et al. Complementary role of ultrasound in management of gestational trophoblastic disease. *Iran J Radiol*. 2015;12:e13955. doi:[10.5812/iranjradiol.13955](https://doi.org/10.5812/iranjradiol.13955).
49. D'Antonio F, Bhide A. Ultrasound in placental disorders. *Best Pract Res Clin Obstet Gynaecol*. 2014;28:429–42.
50. Abdalla N, Bachanek M, Trojanowski S, et al. Placental tumor (chorioangioma) as a cause of polyhydramnios: a case report. *Int J Women Health*. 2014;6:955–9.
51. Fan M, Mootabar H. A rare giant placental chorioangioma with favorable outcome: a case report and review of the literature. *J Clin Ultrasound*. 2014;. doi:[10.1002/jcu.22187](https://doi.org/10.1002/jcu.22187).
52. Prashanth A, Lavanya R, Girisha KM, Mundkur A. Placental teratoma presenting as a lobulated mass behind the neck of fetus: a case report. *Case Rep Obstet Gynecol*. 2012;2012:857230. doi:[10.1155/2012/857230](https://doi.org/10.1155/2012/857230).
53. Nayeri UA, West AB, Grosetta Nardini HK, et al. Systematic review of sonographic findings of placental mesenchymal dysplasia and subsequent pregnancy outcome. *Ultrasound Obstet Gynecol*. 2013;41:366–74.
54. Ohira S, Ookubo N, Tanaka K, et al. Placental mesenchymal dysplasia: chronological observation of placental images during gestation and review of the literature. *Gynecol Obstet Invest*. 2013;75:217–23.
55. Minekawa-Mehandjiev R, Masuda K, Yamamoto K, et al. Placental mesenchymal dysplasia differentially diagnosed from molar pregnancy by 3-D inversion mode rendering: a case report. *J Obstet Gynaecol Res*. 2014;40:284–7.
56. Kuwata T, Takahashi H, Matsubara S. “Stained-glass” sign for placental mesenchymal dysplasia. *Ultrasound Obstet Gynecol*. 2014;43:353–5.
57. Himoto Y, Kido A, Minamiguchi S, et al. Prenatal differential diagnosis of complete hydatidiform mole with a twin live fetus and placental mesenchymal dysplasia by magnetic resonance imaging. *J Obstet Gynecol*. 2014;40:1894–900.
58. Kutuk MS, Ozgun MT, Dolanbay M, et al. Sonographic findings and perinatal outcome of multiple pregnancies associating a complete hydatiform mole and a live fetus: a case series. *J Clin Ultrasound*. 2014;42:465–71.
59. •• Masselli G, Brunelli R, Di Tola M et al. MR imaging in the evaluation of placental abruption: correlation with sonographic findings. *Radiology*. 2011;259:222–30. *Study demonstrates the role of DWI for placental evaluation on MRI*.